

# FINDINGS OF SIMULATION STUDIES FOR THE FAST CORRECTOR MAGNETS OF PETRA IV

J. Christmann\*, L. A. M. D'Angelo, H. De Gersem, TU Darmstadt, Germany  
A. Aloev, S. H. Mirza, S. Pfeiffer, H. Schlarb, M. Thede,  
Deutsches Elektronen Synchrotron (DESY), Hamburg, Germany

## Abstract

Fourth-generation synchrotron radiation sources, which are currently being planned in several accelerator laboratories, require fast orbit feedback systems to correct distortions in the particle orbit in order to meet stringent stability requirements. Such feedback systems feature corrector magnets powered at frequencies up to the kilohertz range, giving rise to strong eddy currents. To understand the eddy current effects and the characteristics of these fast corrector magnets, elaborate finite element simulations must be conducted. This paper gives an overview of the most important findings of our simulation studies for the fast corrector magnets of the future synchrotron radiation source PETRA IV at DESY, Hamburg, Germany. Using a homogenization technique for the laminated yokes, we simulate the magnets over a wide frequency range.

## INTRODUCTION

At DESY in Hamburg, Germany, the design phase of the fourth-generation synchrotron radiation source PETRA IV is coming to an end. This upgrade of the existing storage ring PETRA III will offer an increase in brightness by 2-3 orders of magnitude [1], making it the brightest synchrotron radiation source in the world. To achieve this, the magnetic lattice must provide ultralow electron emittance, which makes orbit position stability a core issue [2]. To that end, a fast orbit feedback system (FOFB) is being designed [3]. The FOFB will feature hundreds of fast orbit corrector magnets powered at frequencies up to the kilohertz range [4]. At such high frequencies, eddy currents in the magnets' laminations have a strong effect on the correctors' characteristics, i.e., the field in the aperture is attenuated and delayed. Thus, accurate finite element (FE) simulations of the eddy current effects are needed. However, the laminated structure of the magnets' yoke and the small skin depths at high frequencies make these simulations cumbersome. To ease the computational effort, we employ a homogenization technique which enables us to simulate the correctors not just as a stand-alone model but also including the neighboring quadrupole magnets.

## SIMULATION PROCEDURE

We conduct 3D frequency domain FE simulations of a magnetoquasistatic problem using CST Studio Suite® [5]. In the magnets' yoke, the conductivity  $\sigma$  and the reluctivity  $\nu$  are functions of the spatial coordinate, since they are different for the conducting laminates and their insulating coating.

The homogenization technique, as proposed in [6], consists in replacing  $\sigma$  and  $\nu$  in the yoke with spatially constant material tensors

$$\begin{aligned} \overline{\overline{\sigma}} &= \gamma \sigma_c \begin{bmatrix} 1 & 0 & 0 \\ 0 & 1 & 0 \\ 0 & 0 & 0 \end{bmatrix}, \\ \overline{\overline{\nu}} &= \frac{\sigma_c d \delta \omega (1+j)}{8} \frac{\sinh\left((1+j)\frac{d}{\delta}\right)}{\sinh^2\left((1+j)\frac{d}{2\delta}\right)} \begin{bmatrix} 1 & 0 & 0 \\ 0 & 1 & 0 \\ 0 & 0 & 0 \end{bmatrix} \\ &+ \nu_c \begin{bmatrix} 0 & 0 & 0 \\ 0 & 0 & 0 \\ 0 & 0 & 1 \end{bmatrix}, \end{aligned}$$

where the yoke is stacked in  $z$ -direction,  $\sigma_c$  denotes the conductivity of the laminates,  $\nu_c$  their reluctivity,  $d$  their thickness, and  $\delta = \sqrt{\frac{2\nu_c}{\sigma_c \omega}}$  is the skin depth. The parameter  $\gamma$  is the percentage of the yoke's volume consisting of conducting material, called "stacking factor". The derivation of the reluctivity tensor is detailed in [6]. A verification of this technique in the context of fast corrector magnets is provided in [7].

## SIMULATION OF A STAND-ALONE CORRECTOR MAGNET

The model of a fast corrector for PETRA IV is shown in Fig. 1. While the shape of the yoke is reminiscent of an octupole magnet, the corrector produces a dipole field. On each of the eight posts pointing to the aperture, there is a thick main coil and a thinner auxiliary coil, only one of which is powered in the simulations. The main coils have 65 turns, the auxiliary coils have 27 turns and both get an AC current with an amplitude of 15 A. The coils that are switched off are shown in grey. If the coils are powered as shown, a vertical field is produced. If the opposite set of coils was powered, a horizontal field would be produced. Note that throughout this paper, we assume the laminations to have a stacking factor of  $\gamma = 0.91$ , a relative permeability of  $\mu_r = 2780$ , and a conductivity of  $\sigma = 6.993 \text{ MS m}^{-1}$ , corresponding to a typical electrical steel such as AISI 1010.

For the design of the feedback system, the integrated transfer function

$$\text{ITF}(f) = \frac{\int_{l_z} B_1(z, f) dz}{\int_{l_z} B_1^{\text{DC}}(z) dz}$$

is of particular interest. Herein,  $B_1(z, f)$  denotes the magnetic dipole coefficient at frequency  $f$  and position  $z$  along

\* jan-magnus.christmann@tu-darmstadt.de

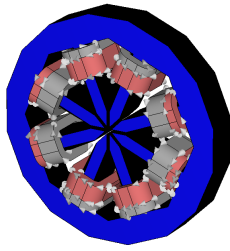


Figure 1: Model of a fast corrector magnet in CST Studio Suite® [5].

the longitudinal axis. Note that this coefficient is computed by transforming the field back into time domain and evaluating at the time instant when the aperture field is at its maximum.  $B_1^{DC}(z)$  is the dipole coefficient in the DC-case and  $l_z$  is interval along which we integrate. The latter must be chosen large enough to capture the stray fields entirely.

The second quantity of interest is the field lag  $\phi$ , i.e., the phase difference between the current in the coils and the aperture field.

### Results for the Model Without Beam Pipe

First, we investigate the model without beam pipe. Figure 2a shows the ITF for a yoke with different lamination thicknesses, Fig. 2b shows the field lag. From Fig. 2a, we can see that the 3 dB bandwidth of the system depends strongly on the lamination thickness. Changing the lamination thickness within a realistic interval from  $d = 0.3$  mm to  $d = 1$  mm, the bandwidth decreases from  $f_{3\text{dB}} = 45$  kHz to  $f_{3\text{dB}} = 5$  kHz, while the field lag at the bandwidth stays constant at roughly  $\phi_{3\text{dB}} = -10$  deg. The latter observation does not mean that the lamination thickness does not influence the field lag. On the contrary, as can be seen in Fig 2b, a larger lamination thickness will cause a significantly larger delay between the current in the coils and the field in the aperture at a given frequency.

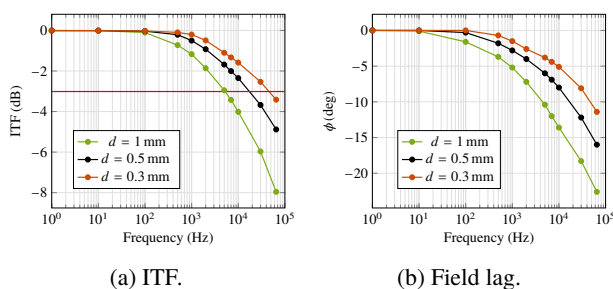


Figure 2: ITF and field lag for different lamination thicknesses.

### Results for the Model With Beam Pipe

Next, we include a beam pipe in the model. The beam pipe is made of AISI 316LN stainless steel, with  $\mu_r = 1.01$  and  $\sigma = 1.351 \text{ MS m}^{-1}$ . It has a circular cross-section with outer radius  $r_{\text{out}} = 11$  mm and a wall thickness of  $b = 1$  mm.

For brevity, we limit the following investigations to a model with  $d = 0.5$  mm. Figures 3a and 3b show the direct comparison to the model without beam pipe. We observe that the eddy currents in the beam pipe cause a substantial reduction of the bandwidth as well as significant additional field lag at the higher frequencies. Both effects depend on the thickness of the beam pipe. Table 1 gives the bandwidth and the phase shift at the bandwidth, for different wall thicknesses. We find that going from  $b = 0.5$  mm to  $b = 1.5$  mm, the bandwidth decreases by 47 % and the absolute value of the phase shift at the bandwidth increases by 25 %.

Given the technical difficulty in achieving a relative permeability as low as  $\mu_r = 1.01$ , we have also analyzed models with values up to 1.2, but we have found that the increased permeability has no significant effect on the quantities of interest. Qualitatively, these findings are in agreement with existing analytical formulae for the transfer function of the beam pipe [8].

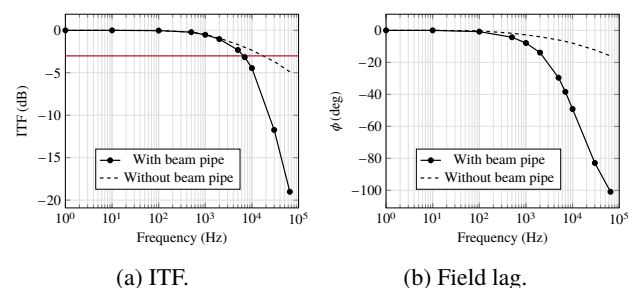


Figure 3: ITF and field lag for the model with and without beam pipe.

Table 1: 3 dB Bandwidth and Field Lag at Bandwidth for Different Beam Pipe Wall Thicknesses

$b$ (mm)	$f_{3\text{dB}}$ (kHz)	$\phi_{3\text{dB}}$ (deg)
0.5	9.8	-32
1	6.6	-37
1.5	5.2	-40

## SIMULATION OF A CORRECTOR MAGNET TOGETHER WITH NEIGHBORING QUADRUPOLE MAGNETS

In the magnetic lattice of PETRA IV, the fast corrector magnets will be placed between two quadrupole magnets (PQB and PQC), see Fig. 4. Differently from the corrector, the quadrupoles are powered by DC currents and their yokes are not laminated. For details on the quadrupole magnets, see [9]. As usual in fourth-generation light sources, the magnetic lattice is very crowded [10], i.e., the distance from the quadrupole yokes to the corrector yoke is only about 11.5 cm. Hence, cross-talk must be investigated.

## Results for the Model Without Beam Pipe

We start the investigation of the cross-talk with a model that does not include a beam pipe. Figure 5a shows the ITF for the model with the quadrupoles in direct comparison to the ITF for the model without the quadrupoles. We find that including the neighboring quadrupoles into the simulation model leads to a peak of up to +0.7 dB in the ITF at lower frequencies.

The reason for the observed peak in the ITF is that the AC field of the corrector induces eddy currents in the non-laminated quadrupole yokes, which then lead to a parasitic dipole component inside the aperture of the quadrupoles. This can be seen in Fig. 5b, where we show the dipole coefficients along the longitudinal axis for the static case and for the time harmonic case with  $f = 10$  Hz. Since the dipole field inside the corrector is not decreasing significantly in the low frequency regime below 100 Hz, this parasitic dipole component leads to an increase in the value of the integrated field compared to the static case. Note that if the quadrupole magnets are modeled with laminated yokes, the eddy currents are suppressed and the parasitic dipole component and consequently the peak in the ITF disappear.

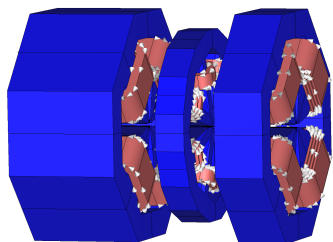


Figure 4: Model of the corrector magnet with the neighboring quadrupole magnets to the left and right in CST Studio Suite® [5].

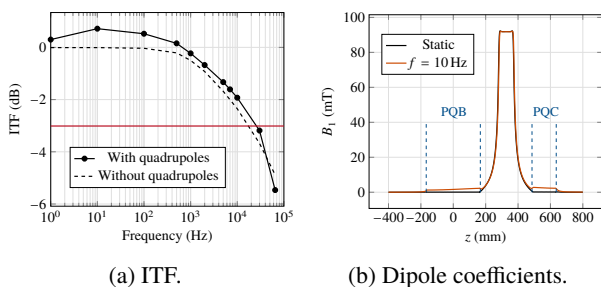


Figure 5: ITF and dipole coefficients along the axis for the model with neighboring quadrupoles without beam pipe.

## Results for the Model With Beam Pipe

Next, we investigate if the inclusion of the beam pipe leads to additional cross-talk. The beam pipe has the same material properties as in the stand-alone model and the wall thickness is  $b = 0.5$  mm.

Figures 6a and 6b show the ITF and the field lag for the magnet with a beam pipe with and without the neighboring

quadrupoles. We again observe differences only in the low frequency regime in the form of a peak in the ITF. The figures also show the results for the model with the quadrupoles but without the beam pipe. We see that in the low frequency regime, where the cross-talk shows its effect, there is essentially no difference to the model without the beam pipe. Therefore, we conclude that the beam pipe does not cause any additional cross-talk.

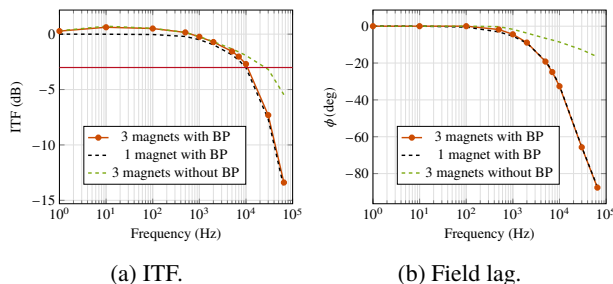


Figure 6: ITF and field lag for model with quadrupoles and beam pipe compared to other models.

## CONCLUSION

In this work, we have presented an excerpt of the simulations which we have conducted for the fast orbit corrector magnets for PETRA IV. We have observed that the lamination thickness of the yoke and the wall thickness of the beam pipe are key parameters and we have quantified their influence on the magnets' bandwidth and the field lag. Moreover, we have found that cross-talk with the neighboring quadrupoles leads to an unexpected peak in the transfer function at lower frequencies, which could be prevented if the quadrupoles would be laminated. Further, we have shown that the cross-talk is not influenced by the beam pipe.

## ACKNOWLEDGEMENTS

We acknowledge the support from Deutsches Elektronen-Synchrotron DESY and the Deutsche Forschungsgemeinschaft (DFG) - Project-ID 264883531 - GRK 2128 "Accelerence". Furthermore, we thank Dassault Systèmes for providing the CST Studio Suite® license.

## REFERENCES

- [1] C. G. Schroer *et al.*, "The synchrotron radiation source PETRA III and its future ultra-low-emittance upgrade PETRA IV", *Eur. Phys. J. Plus*, vol. 137, no. 12, p. 1312, Dec. 2022. doi: 10.1140/epjp/s13360-022-03517-6
- [2] S. Shin, "New era of synchrotron radiation: fourth-generation storage ring", *AAPPS Bull.*, vol. 31, no. 1, p. 21, Aug. 2021. doi: 10.1007/s43673-021-00021-4
- [3] S. H. Mirza, B. Dursun, H. T. Duhme, S. Pfeiffer, S. Jablonski, and H. Schlarb, "Lattice-based simulations for the fast orbit feedback system of PETRA IV", in *Proc. IPAC'23*, Venice, Italy, May 2023, pp. 3989-3991. doi: 10.18429/JACoW-IPAC2023-THPA022
- [4] C. G. Schroer *et al.*, "PETRA IV: upgrade of PETRA III to the ultimate 3D X-ray microscope. Conceptual design report",

- DESY, Hamburg, Germany, Nov. 2019.  
doi:10.3204/PUBDB-2019-03613
- [5] CST Studio Suite, 2023. <https://www.3ds.com/products-services/simulia/products/cst-studio-suite>
- [6] P. Dular, J. Gyselinck, C. Geuzaine, N. Sadowski, and J. P. A. Bastos, "A 3-D magnetic vector potential formulation taking eddy currents in lamination stacks into account," *IEEE Trans. Magn.*, vol. 39, no. 3, pp. 1424-1427, May 2003.  
doi:10.1109/TMAG.2003.810386.
- [7] J. Christmann *et al.*, "Finite element simulation of fast corrector magnets for PETRA IV", *J. Phys. Conf. Ser.*, vol. 2687, no. 8, p. 082010, Jan. 2024.  
doi:10.1088/1742-6596/2687/8/082010
- [8] B. Podobedov, L. Ecker, D. Harder, and G. Rakowsky, "Eddy current shielding by electrically thick vacuum chambers", in *Proc. PAC'09*, Vancouver, BC, Canada, May 2009, paper TH5PFP083, pp. 3398-3400.
- [9] J. Keil, I. Agapov, A. Aloev, R. Bartolini, and M. Thede, "Cross-talk between magnets in the H6BA-cell of PETRA IV", in *Proc. IPAC'23*, Venice, Italy, May 2023, pp. 3624-3627. doi:10.18429/JACoW-IPAC2023-WEPM032
- [10] G. L. Bec, J. Chavanne, S. Liuzzo, and Simon White, "Cross talks between storage ring magnets at the Extremely Brilliant Source at the European Synchrotron Radiation Facility," *Phys. Rev. Accel. Beams*, vol. 24, no. 7, p. 072401, Jul. 2021.  
doi:10.1103/PhysRevAccelBeams.24.072401